Hindawi Publishing Corporation
Advances in Optical Technologies
Volume 2012, Article ID 530512, 12 pages
doi:10.1155/2012/530512

Review Article

Cross-Shaped Terahertz Metal Mesh Filters: Historical Review and Results

Arline M. Melo,[1] Angelo L. Gobbi,[2] Maria H. O. Piazzetta,[2] and Alexandre M. P. A. da Silva[3]

[1] *BR Labs Ltd., Rua Lauro Vannucci 1020, 13087-548 Campinas, SP, Brazil*
[2] *Brazilian Synchrotron Light Laboratory, Rua Giuseppe Maximo Scolfaro, 10000, 13083-970 Campinas, SP, Brazil*
[3] *Department of Microwave and Optics, University of Campinas, (UNICAMP), Avenue Albert Einstein, 400, Cidade Universitária Zeferino Vaz, 13083-970 Campinas, SP, Brazil*

Correspondence should be addressed to Arline M. Melo, armame@gmail.com

Received 5 October 2011; Revised 27 December 2011; Accepted 10 January 2012

Academic Editor: Michael Fiddy

Copyright © 2012 Arline M. Melo et al. This is an open access article distributed under the Creative Commons Attribution License, which permits unrestricted use, distribution, and reproduction in any medium, provided the original work is properly cited.

Terahertz frequencies experiments has motivated the development of new sources, detectors and optical components. Here we will present a review of THz bandpass filters ranging from 0.4 to 10 THz. We also demonstrate our fabrication process, simulations and experimental results.

1. Introduction and Review

1.1. Basic Concepts. The terahertz, or far infrared range within electromagnetic spectrum placed between microwaves and midinfrared wavelengths, correspond to wavelengths from 3 millimeters up to 3 micrometers. Moreover, the transition between these two spectral bands represents the transition of two different technologies: electronics and photonics (Figure 1). These issues bring us technological challenges to develop new sources, detectors, filters, and other important components [1, 2].

Recently, terahertz range has attracted the interest around the world because its innovative applications including different areas as nondestructive tests, military and civilian security, chemistry, medicine, biology, and others [3–6]. Especially after terrorist attacks on September 11th, terahertz research has increased abruptly because all possible defense applications.

THz radiation can be transmitted through different materials, which became possible to "see" through clothes, shoes, bags, plastics, and paper envelops, allowing the identification of chemical and biological agents like illicit drugs and explosives [3, 5].

1.1.1. Terahertz Metal Mesh Filters. A metal mesh filter, which is a type of frequency selective surfaces (FSS), can be defined by a thin metal film (few to tenths of microns of thickness) which is perforated, using different geometries, in a two-dimensional array. These filters are compact and present an easy and available fabrication process. They also could act as high pass, low pass, band-pass, or reject band filters and this is the most important characteristics of them in other words, their optical behavior can be changed selecting the proper geometry and their parameters dimensions [7].

There are some examples of FSS geometries in the literature presenting different spectral response. In Figure 2, it shows few examples of band pass, high pass, and reject band filters.

The most known band pass geometry is the cross-shaped (see Figure 3) where the frequency profile is determined by the dimensions of the crosses width (K), length (L), and periodicity (G) (Figure 3).

The main fabrication process used to produce metal mesh filters is the photolithography, where a substrate is prepared to receive a photoresist (polymer sensitive to light—UV is the most common radiation used). After the deposition of this polymer, the sample has to be baked and then exposed to a light source using a mask with the geometric patterns. The light will pass through the transparent areas on the mask substrate and interact with the photoresist. In this step, the sample will receive other bake phase followed by the development process of photoresist. Finally the sample

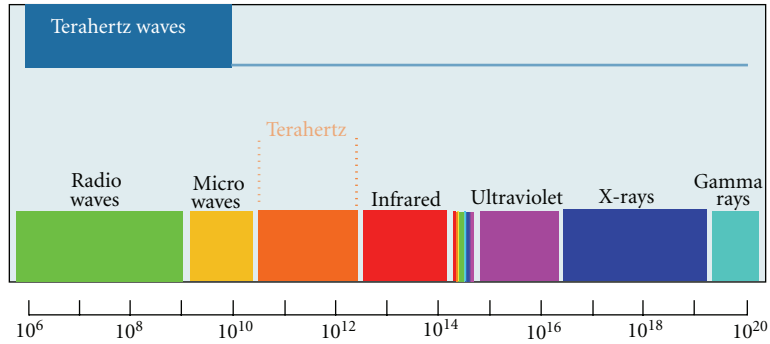

Figure 1: Electromagnetic spectrum showing the terahertz range between microwaves and infrared ranges.

is ready to the metal deposition, where the thin film will be evaporated or growed in a metallic bake.

Although conventional photolithography is the most common fabrication process, we can cite few other techniques as direct write using electron beam (Direct Electron Beam Litography, DEBL), nanoimprint and laser ablation [8–10]. Figure 4 shows the results for cross-shaped filters obtained using different fabrication process.

1.1.2. Metal Mesh Filters Applications. The metal mesh filters can be applied in different areas and here we will cite some applications examples cited in the literature:

(i) Astronomy. Infrared astronomy can be possible using satellites and airborne telescopes operating within the whole infrared range and at high-altitude sites, where the observations are affected primary by water vapor atmospheric absorption. There are some atmospheric windows (25 and 38 microns at sites higher than 5000 m) where it is still possible to observe extraterrestrial sources with lower losses. Long midinfrared ranged from 25 up to 40 microns, allows observing reddened sources and different molecular/atomic lines and dusting features [11].

(ii) Free Electron Lasers. Different quasioptical components, including metal mesh filters, are applied as passive selective components (filters) on experiments using terahertz-free electron lasers as the NovoFel at Novosibrisk [12]. These devices should be able to operate over a long period of time under high-power conditions without important degradation of their properties [12].

(iii) Imaging. Other potential applications are related to infrared imaging and spectroscopy, which are related also to the devolpement of high power terahertz sources and high sensitivity detectors within these wavelength range [13].

(iv) Energy-Saving Glasses. In other dimension scale (millimeters), cross-dipole FSS can be used to generate energy-saving glasses, which can be applied on buildings to keep them cooler during summer and warmer during winter. It also allows the reception of useful microwave/RF signals required for mobile phone, GPS, and personal communication systems. This application is possible using mm-wave metal band-pass filters, which block all infrared wavelengths and transmit the desired mm-waves frequencies [14].

(v) Sensors. Bolometer sensors and cameras are very useful to detect infrared radiation and their performance can be improved by the incorporation of FSS elements with no requirement for external filters to define the absorbing band [15].

1.2. Historical Review and Results. Ulrich [16] is one of the most cited articles about metal mesh filters. In this work, a metal mesh interference filter is used to replace the output coupler of a far infrared molecular laser. This interference filter consists of two parallel reflector grids with a large array of small coupling holes where the reflectance is varied by adjusting the spacing between the grids. Ulrich also was one of the responsibles for showing that the transmission properties of these metallic meshes could be considered as circuit elements on a free space transmission line. Using this theory, it is possible to determine the transmission profile of inductive (square openings) and capacitive (free-standing squares) meshes, high pass and low pass, respectively.

After these first experiments and theoretical approaches, one can find in the literature many other authors who fabricated and tested band pass metal mesh filters at different sub-THz and THz frequencies. It is shown in Table 1 different experimental results found in the literature, which are just a few of the total works about band pass metal mesh filters published until now. In this table, it is also presented the grid parameters of several filters designed to operate within the range from 100 GHz up to 14 THz, exhibiting high-transmission peaks and band pass widths between 13 up to 50% of the central frequency.

The freestanding filters present a high mechanical fragility. Then, some authors have used photolithography process over some support material, p. e. Mylar (polyester film), polyamide, teflon (polytetrafluoroethylene), and others, which are semitransparent within those frequencies range.

Recently, other interesting works have been published using different materials as substrate, such as Polymethylpentene (TPX), TydexBlack, and high-density polyethylene (HDPE). The use of these materials could become a very

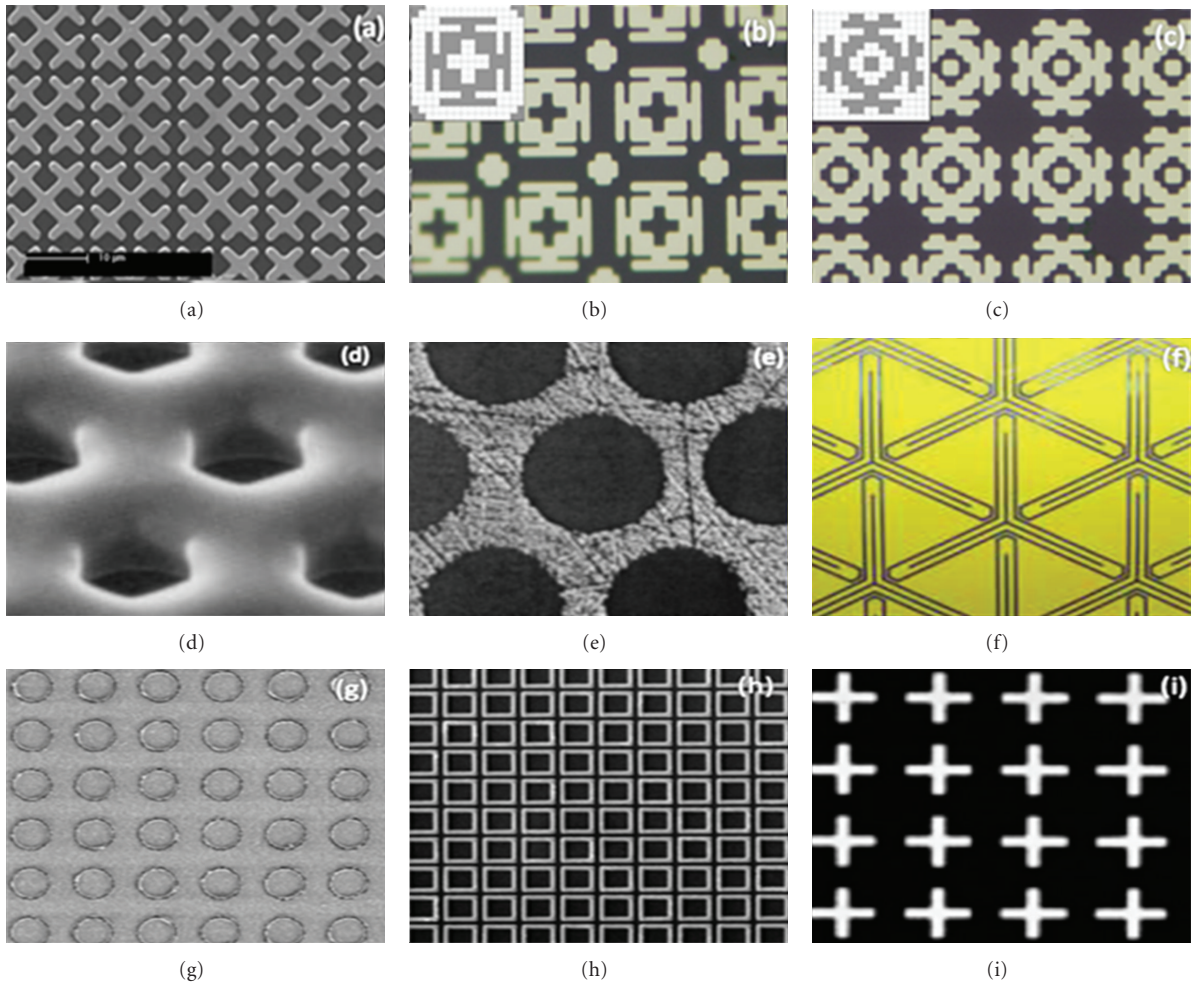

Figure 2: Examples of filters presented in literature: (a) reject band peak at 6.9 and 20.3 THz; (b) reject band peak at 3.8 and 7.0 THz; (c) reject band peak at 2.7 and 5.9 THz [20]; (d) band pass filter at 1.7 THz; (e) high-pass filter at 1.1 THz [21]; (f) blocking of multiple frequency bands [22]; (g) band pass at 7 microns [23]; (h) band stop sample [24]; (i) band pass sample [12].

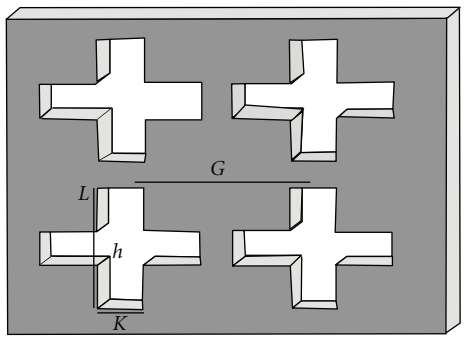

Figure 3: Dipole cross-shaped band pass filter parameters.

important way to fabricate useful filters because they can also act as a high-pass filter for wavelengths above near infrared (NIR: 1–20 microns). In this case, it would be very helpful to applications where the background radiation in these wavelength range (visible and NIR) is prohibitive.

The transmission profiles for TydexBlack, TPX, and HDPE are shown in Figure 5.

In Kaufmann et al. [17], different filters at 2.4 THz have been fabricated using THz semitransparent materials as substrate. In this work, it is compared the transmission profile obtained by a suspended metal mesh, a filter on a TydexBlack base, and by a metal mesh sandwiched between TPX layers. The results have shown a high transmittance for the suspended filters, as expected. The measurements resulted in a 40% and 48% transmission for the filter with TydexBlack and the TPX sandwiches, respectively. They also concluded, in the same work, that the transmission is independent from the polarization position angle and the dependence on the incidence angle becomes more important for angles larger than 20 degrees.

Ma et al. [13] also developed similar filters using low-loss substrate material, high-density polyethylene (HDPE). Filters for three different frequencies were fabricated, 1.5, 1.75 and 2.91 THz, using photolithography process above a 1 mm thick HDPE plate. The measured transmission resulted

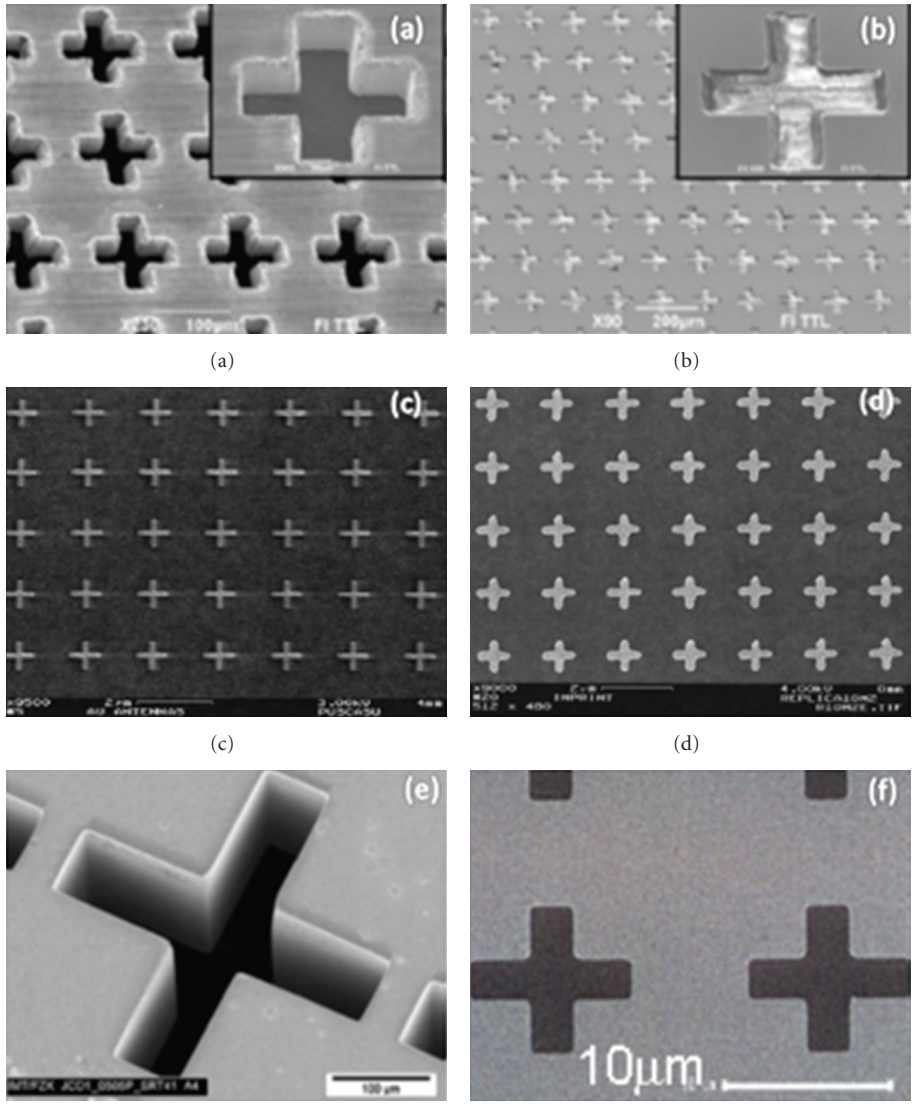

Figure 4: Electron microscopy images illustrating the structural results for different fabrication process: (a) laser ablation-free standing [8]; (b) laser ablation-on a support material standing [8]; (c) DEBL [9]; (d) Nanoimprint [9]; (e) X-ray photolithography [10]; (f) UV photolithography [11].

in 51%, 54%, and 52%, for the 1.5, 1.75, and 2.91 THz, respectively.

2. Our Contribution

The second part of this chapter intends to present our contribution to this topic. We will review all important job achievements published in 2008 [18] and continue with more recent developments of our group.

2.1. Project of Different Band Pass Filters between 0.5 and 10 THz. The initial motivation to design band pass filters to these specific frequency range came from an astrophysical application, Solar Physics, and especially solar flares. There are two different ways to observe the Sun, from the ground and using balloons or satellites outside our atmosphere. Observations through our atmosphere are limited by the water vapor column presented in the observation site. There are, within the terahertz range, three atmospheric windows (which are known as frequency regions within the electromagnetic spectrum presenting absorption coefficient minimums) centered at 405, 670, and 850 GHz. The other higher frequencies filters were designed considering outside-atmosphere observations [19].

All filter parameters designed here are based on Porter-field work. Considering linear variation of the mesh parameters (K, L, and G) we calculate a conversion factor for each parameter which will be used to design other frequencies filters as below, in Table 2.

Using the conversion factors shown in Table 2, we are able to calculate new parameters mesh in order to have

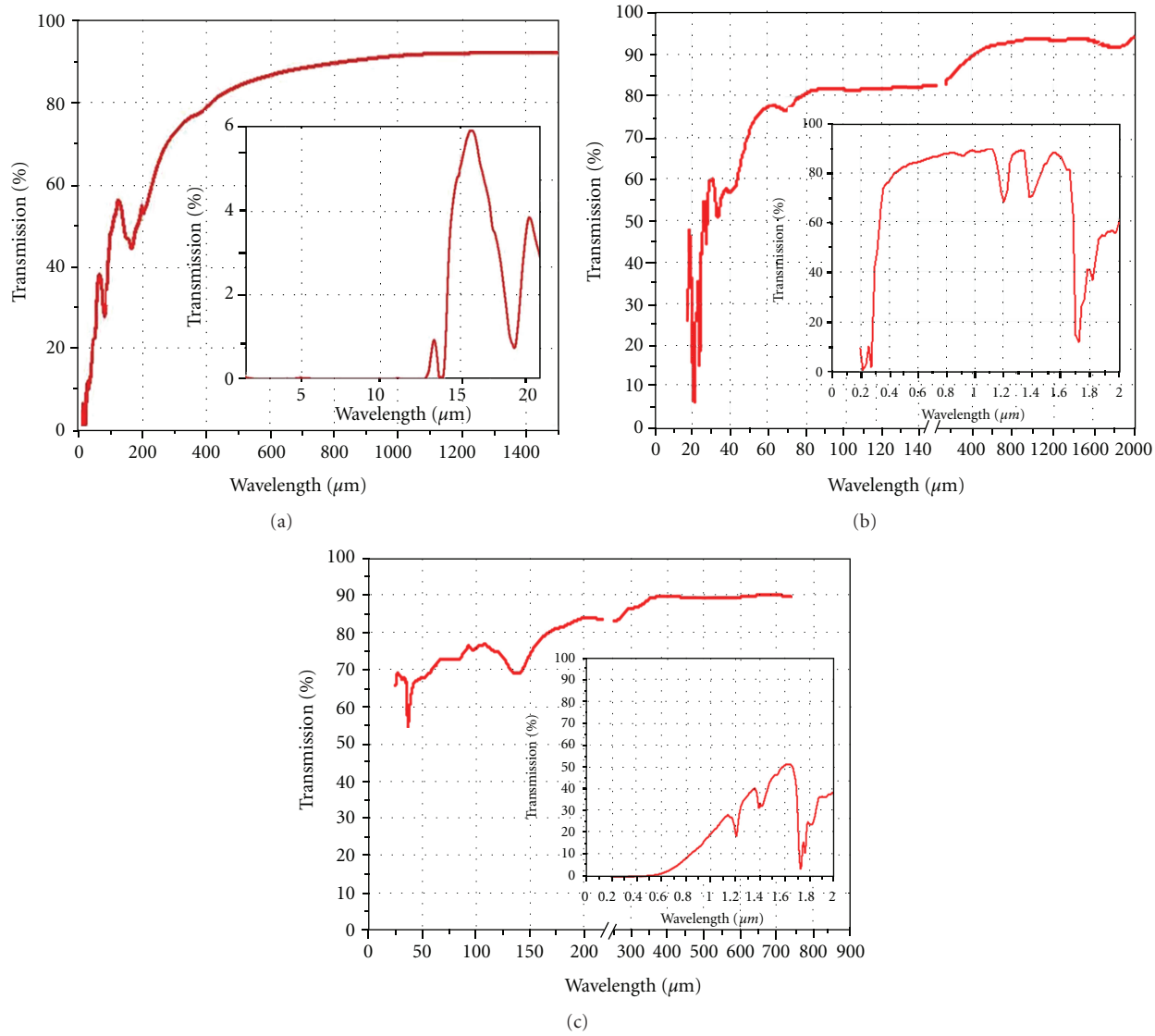

Figure 5: Transmission profile for: (a) TydexBlack, (b) TPX, and (c) HDPE by Tydex company measurements.

a new band pass filter just multiplying the factor by the desired central wavelength in microns. In Table 3, it is shown our calculated parameters dimensions for filters operating from 0.4 up to 10 THz. As Porterfield filters presented a band pass width about 15% of the central frequency, all filters design using this method will generate filters with bandwidths around the same value. As you can see in Table 3, we also designed filters to present double bandwidths, 30% of central frequency, and in this case we used simulation methods.

Using a commercial electromagnetic simulator code, CST microwave studio, we could calculate in a good approximation the mesh parameters for filters with larger bandwidths. In this case, we have calculated the initial mesh parameters values for narrow bandwidth (15%) considering the conversion factors presented here. In the optimization process, it was determined, as the software goals, to achieve at least the desired new bandwidth and that the resonant frequency remained the desired central frequency. At the end of optimization process, CST has returned the new parameters dimensions. We have fabricated and measured these larger bandwidth filters, proving that this can be an easy and effective technique to design filters presenting new bandwidth values (Figure 6).

2.2. Fabrication Process: Photolithography and Metallic Deposition. Filters such as the presented ones can be fabricated using different techniques. One micromachining technique uses polymer film as substrate with a metallic thin layer deposited on one side (e.g., Mylar). However, plastic films add absorption and have thermal and mechanical limitations for certain applications.

Another micromachining procedure, known as LIGA, explores photolithography followed by electroplating techniques, producing a metal grown film with open space cross formats, without absorption, which improves the final filter

Table 1: Band pass metal mesh filters results from different authors.

Author	Frequency (THz)	G (microns)	K (microns)	J (microns)	Transmission (%)	Bandpass width (%)	Fabrication process
Page [25]	0.138	972	892	28	91	35	Mylar photolithography
Page [25]	0.174	842	762	35.5	85	41	Mylar photolithography
Page [25]	0.282	504	444	22.5	92	46	Mylar photolithography
Page [25]	0.384	438	288	7.5	72	17	Mylar photolithography
Page [25]	0.480	376	226	11.5	66	16	Mylar photolithography
Page [25]	0.510	286	226	15	78	33	Mylar photolithography
Porterfield [7]	0.587	402	251	66	97	17.3	Free UV photolithography
Porterfield [7]	1.195	201	126	33	100	16.9	Free UV photolithography
Ma [13]	1.5	106.3	81.4	22.6	51	40	HDPE photolithography
Porterfield [7]	1.523	154	98	28	97	18.6	Free UV photolithography
Ma [13]	1.77	76.5	66.4	12.6	54	51	HDPE photolithography
Porterfield [7]	2.084	113	71	19	100	15	Free UV photolithography
Ma [13]	2.91	60	38	10	52	13.7	HDPE photolithography
Kuznetsov [12]	3.75	41.4	29.4	6	59	30	Polyimide LIGA*
Kuznetsov [12]	6.5	28.5	18.5	5	64	30	Polyimide LIGA*
Smith [26]	7.9	22	12.8	3.5	52	15	Polyimide Optical photolithography
Möller [27]	8.3	26.4	23.2	2.4	50	14	Free UV photolithography
Möller [27]	13	16.7	14.7	1.5	60	17	Free UV photolithography
Möller [27]	14	16.4	13.9	2.5	80	23	Free UV photolithography

*LIGA is a german acronym for Lithography, Electroplating and Molding.

Table 2: Mesh parameter conversion factors.

Porterfield et al. [7] $K = 261$, $L = 76$, and $K = 402$ micrometers; $f = 0.585$ THz ($\lambda = 512.8$ micrometers)		
K parameter conversion	L parameter conversion	G parameter conversion
Ck = 261/512.8 = **0.50897**	Cl = 76/512.8 = **0.1482**	Cg = 402/512.8 = **0.78393**

transmission. We used the second technique to fabricate filters with frequencies centered between 0.4 and 10 THz.

We used silicon substrates previously prepared with deposited films of SiO_2, Ti, and Au. The lithography has used SU-8, deposited at 1000 rpm during 30 seconds, for filters frequencies below 2 THz, and at 1500 rpm during 30 seconds, for the higher frequency filters.

The obtained samples were submitted to a baking process, then exposed to UV radiation during 30–40 seconds and finally developed. This process sequence prepares the samples for the deposition of the metallic material, nickel in our case, which is finally the material of the filter, Figure 7.

The electroplating process used a WATTS bath of nickel sulfate, nickel chlorine, boric acid, and water, with current density of 3 A/dcm^2. The last step is the etching, to remove the photoresist and the layers of SiO_2, Ti, and Au using potassium cyanide and HF buffer.

2.3. Microscopic Characterization. After all fabrication process, the next step is an initial characterization of the filters. We usually submit all samples to an optical inspection using a 50x microscope, where we could evaluate defects which affect a region of the filter. As the second step, we are interested to measure the grid parameters to compare with the designed dimensions and evaluate the crosses profiles imperfections. Figure 8 shows good pattern results obtained for 0.67, 1.5, 3, and 4 THz filters.

During the fabrication process, different imperfections could appear in your sample. In Figure 9, we are illustrating a few of them.

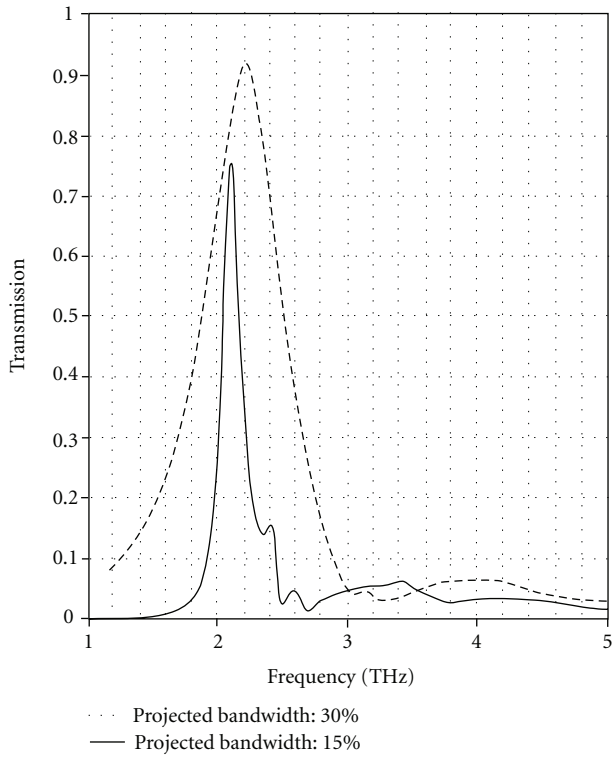

Figure 6: Comparison between measured transmission profiles for the designed band pass filter centered at 2 THz with 30% and 15% bandwidths.

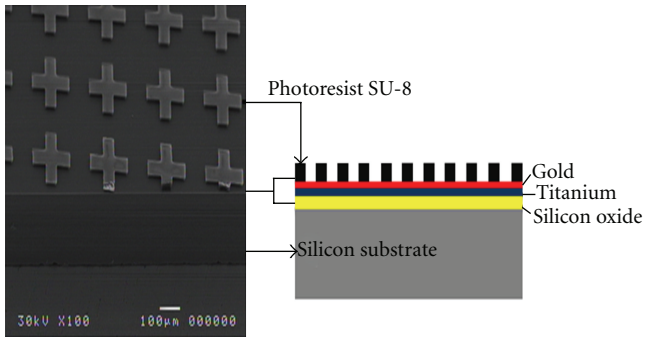

Figure 7: SEM micrograph of a sample after the photolithography process. In this image the thick SU8 crosses prepare the sample to the metallic deposition step.

As the filter frequency increase, the metal thickness has to decrease to avoid a waveguide process. For example, considering the 10 THz filter (corresponding to 30 micrometer wavelength), the filter thickness needs to be less than 10 microns. We adopt free standing filters to avoid the high absorption of any support material and in this case the fabrication process of a very thin metallic film is very sensitive to the mechanical stresses. Figure 9(a) depicts the crack of a 7-micron thick film.

Figures 9(b) and 9(d) shows rounded cross shaped profile examples. In these cases, imperfections are related with the photolithography process, especially with the UV exposition

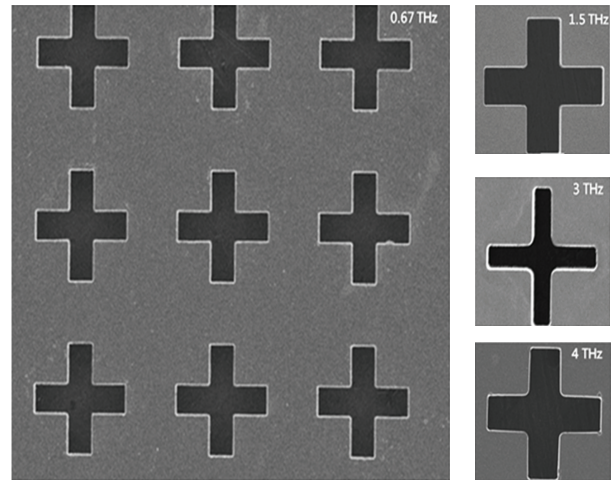

Figure 8: SEM images for different band pass filters frequencies.

Table 3: Mesh parameter designed to band pass filters operating between 0.5 and 10 THz.

Frequency	k (μm)	j (μm)	g (μm)	Expected bandwidth
405 GHz	370	110	590	15%
670 GHz	225	60	350	15%
850 GHz	175	50	302,5	15%
1 THz	153	44.5	235	15%
1.5 THz	102	30	157	15%
2 THz	76	22	120	15%
2 THz	81.4	22.6	106.3	30%
3 THz	66.4	12.6	76.5	30%
4 THz	38	10	60	15%
6 THz	25	7.4	39	15%
8 THz	19	5.6	29.4	15%
10 THz	3.2	15.4	22.5	15%

time of the SU8 resist and its development process. The resist time exposition has to be very precise and be tested along the process because, if we use less radiation doses the resist corner details could not be sensitized and during the development process the SU8 material will be removed.

Figure 9(c) illustrats a growth metallic film presenting a difference in rounded corner. It could happen if the metallic film is growth until the top of the SU8 crosses. It is explained because the facts that during the development phase the first resist layer started to be removed and the resist profile became rounded at the top. There is a simple empirical rule where the metal film is growing using just 80% of the thickness of the resist crosses.

2.4. THz Transmission Measurements. Figure 10 presents the transmission profiles for seven filter samples measured using a Fourier transform infrared spectroscopy (FTIR). It is shown in Table 4 the measured central frequencies, bandwidths, and transmission percentages for the filters in

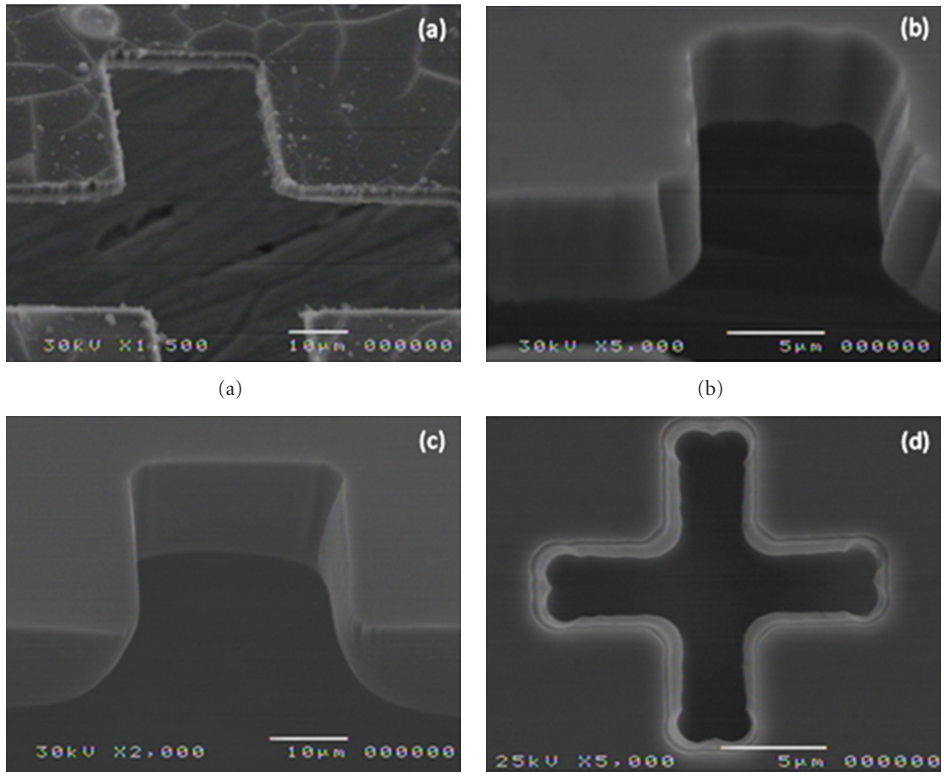

(a) (b) (c) (d)

Figure 9: SEM images illustrating different defects by the fabrication process.

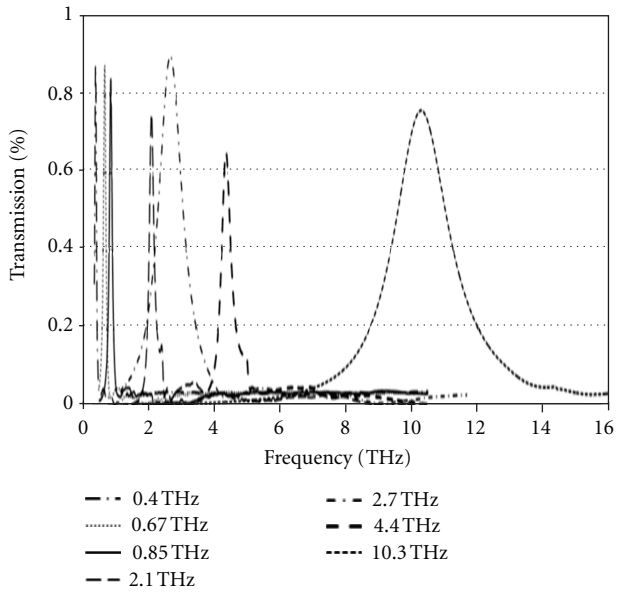

Figure 10: Transmission profile for filters designed between 0.4 and 10 THz measured using the Fourier Transform Infrared Spectroscopy (FTIR) technique.

Figure 10. We can see that the results presented are in accordance with the designed central frequency and bandwidth as shown in Table 3.

Table 4: Measured central frequency, bandwidth, and transmission for filters presented in Figure 10.

Frequency	Measured frequency	Bandwidth (% Fc)	Transmission (%)
405 GHz	395	17.6	88
670 GHz	674	14.2	87
850 GHz	858	14	84
2 THz	2.1	10.7	75
3 THz	2.7	28.5	90
4 THz	4.4	8.8	67
10 THz	10.3	13.9	76

The Figure 11 presents the transmission profile comparison between FTIR measurements and our simulated data obtained using the CST software. The data show a good agreement between simulated and experimental results, validating the simulation technique to support new filters design.

2.5. Simulations. Here we are presenting, using only simulations results, the effect of the individual variation of each mesh parameter on the expected resonant frequency and bandwidth. It will give us an insight about what can happen due to small errors caused by fabrication process. In order to compare the designed filters presented in Table 3 on the same graph, each filter has its frequency range normalized

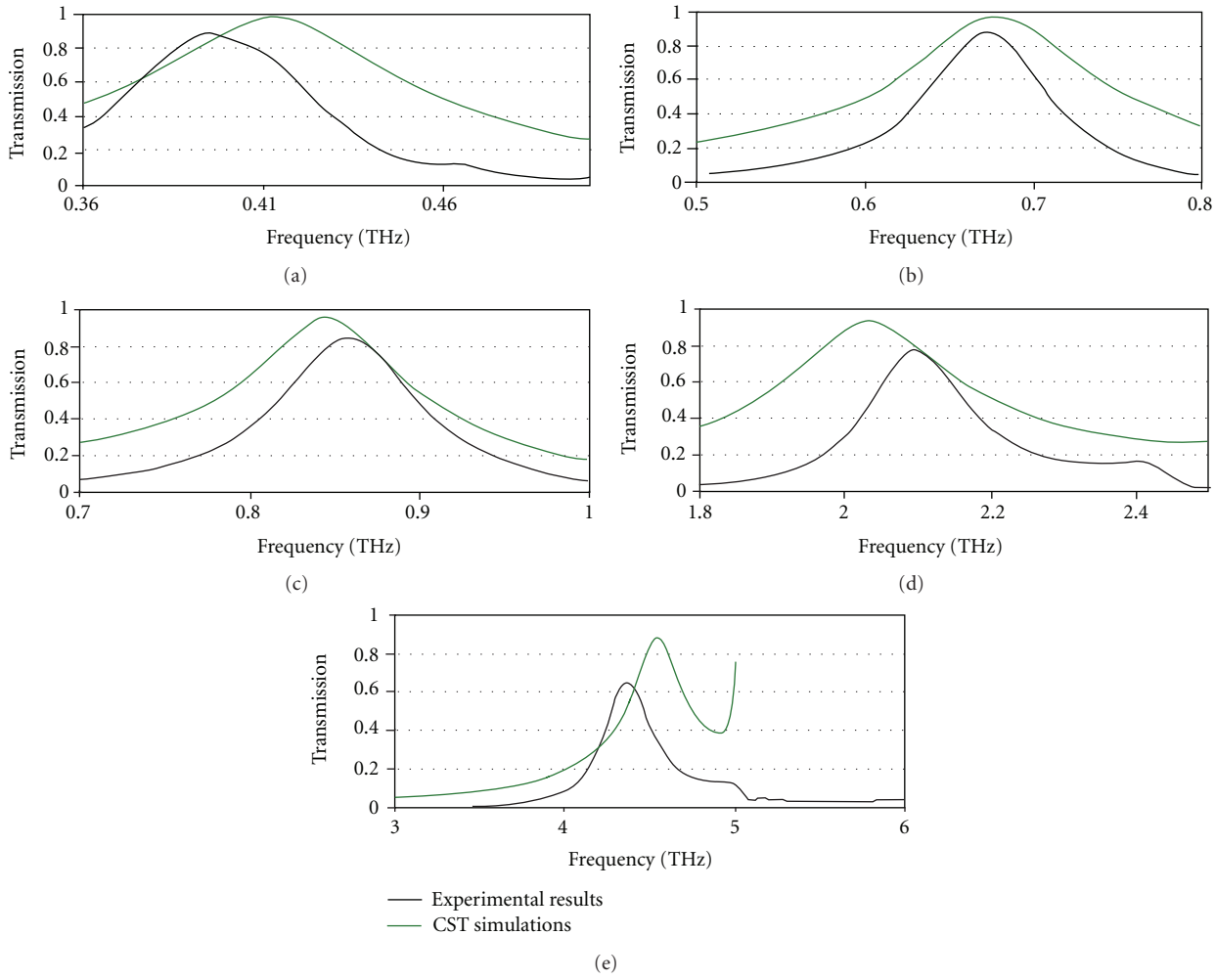

Figure 11: Comparison between the measured transmission profile and the simulated data from CST software for filters at 0.4, 0.67, 0.85, 2, and 4 THz.

by its own peak frequency. Following the same method, the range of variation for all parameters is also normalized by the designed values.

In Figure 12(a), it is shown that the variation on the periodicity, parameter G, can linearly shift the peak frequency up or down. In a general way, if parameter G increases, the peak frequency decreases and vice-versa. However, for a variation of up to 20%, the peak frequency suffers a shift no bigger than 10%. In Figure 12(b), one can note that bandwidth is affected in a nonlinear way, increasing by the decrease of parameter G or decreasing by the increase of parameter G.

A different behavior is observed on the variation of parameter K. In Figure 13(a), it is shown that increasing K, the peak frequency is also increased almost linearly. However, for a variation of up to 20%, the peak frequency shifts no more than 2.5%. The same almost linear effect is seen on bandwidth when parameter K is increased.

Parameter L presents the strongest influence on the peak frequency position, as can be seen in Figure 14 (a). For a variation of up to 20%, the central frequency is shifted more than 10%. Similarly to parameter G, if L is increased, the peak frequency decreases and vice-versa. However, parameters G and L have opposite behaviors regarding bandwidth, when parameter L is increased, bandwidth is also increased but almost linearly.

Another common pattern profile issue caused by fabrication process is rounded corners. In this case, the crosses arms corners are not sharp as designed. Here, this error will be taken into account by the variation in the radius R at the filter's corners as depicted in Figure 15.

In order to compare filters, it is defined as the corner error, the relation of R and parameter L. The maximum corner error is 50%, where $R = L/2$. It is shown in Figure 16 that increasing R, the peak frequency is shifted to higher frequencies up to 10% of the central frequency. The result regarding bandwidth is not conclusive, presenting almost no measurable variation for higher frequencies.

3. Conclusion

3.1. THz Filters Companies. Currently, we find some companies which can fabricate and sell different terahertz metal

Table 5: Terahertz metal mesh filters companies.

Company	Filter type	website
BR-labs	Bandpass filter between 0.4 to 10 THz or custom made.	http://www.br-labs.com/
QMC instruments	Low pass filter with edges between 0.3 to 20 THz.	http://www.terahertz.co.uk/
Virginia diodes	Bandpass filter between 0.35 to 5 THz or custom made.	http://www.vadiodes.com/
Mutsumi corporation	Bandpass filter between 0.2 to 2 THz.	http://www.science-mall.co.jp/en

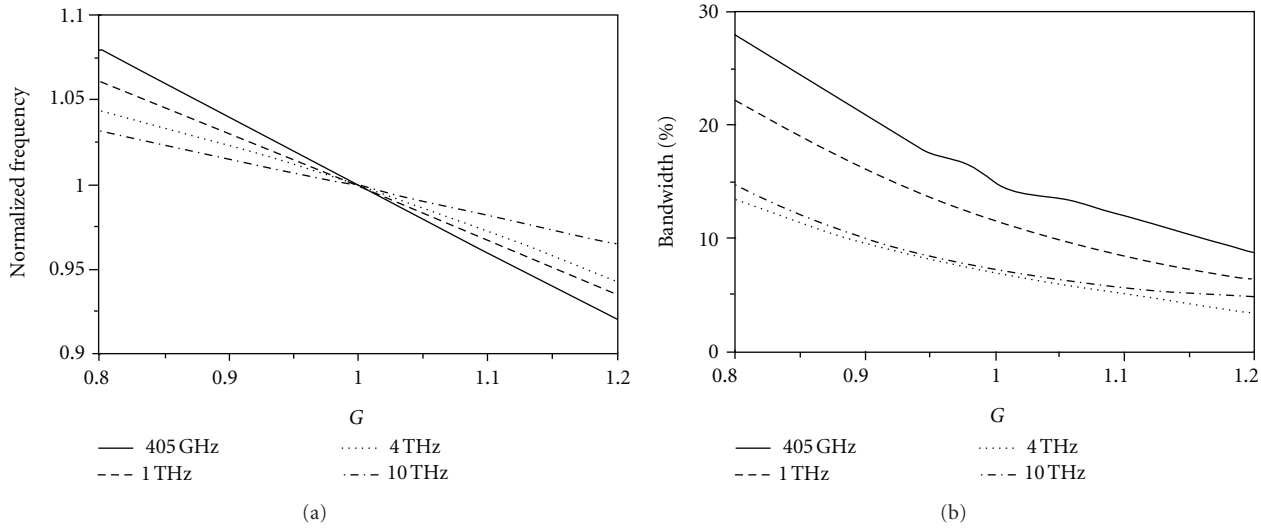

Figure 12: Effect of parameter G variation on (a) resonant frequency, (b) bandwidth.

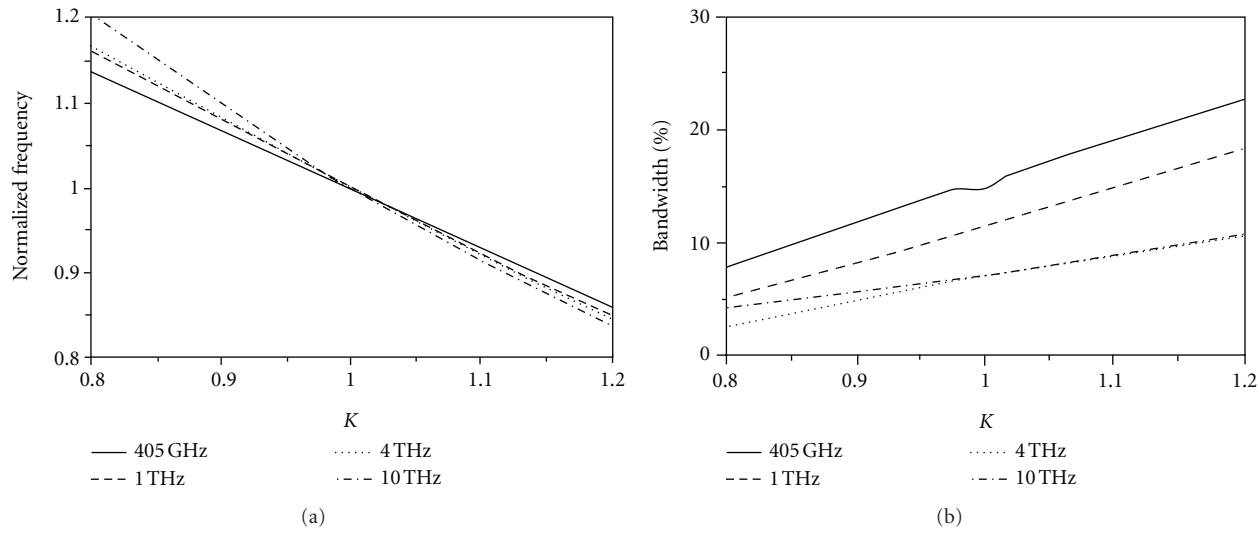

Figure 13: Effect of parameter K variation on (a) resonant frequency, (b) bandwidth.

mesh filters (high-pass, low-pass, and band pass transmission). The available frequencies for band pass filters are between 200 GHz up to 10 THz, and the prices are around USD 2.000 up to USD 10.000, varying if the item is in stock or will be custom made. In Table 5 it is presented four examples of companies.

3.2. Conclusions. In this chapter we presented a brief introduction to important concepts and definitions for terahertz and metal mesh filters areas, including the most common applications to both topics. A compact historical review of bandpass filters works is also presented. In the second part of this work we approach our own contributions on

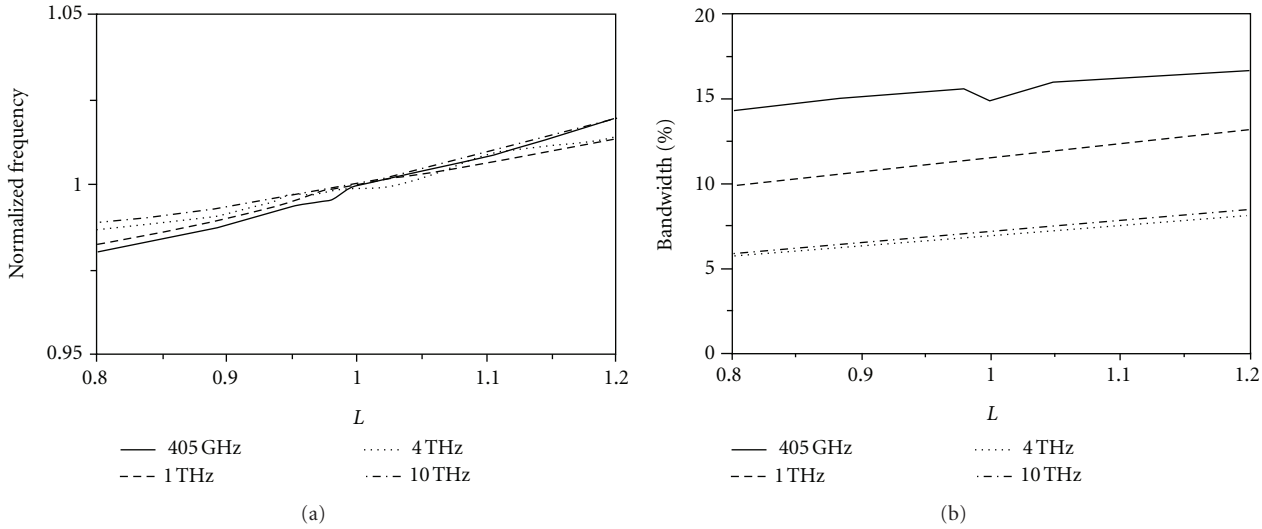

Figure 14: Effect of parameter L variation on (a) resonant frequency, (b) bandwidth.

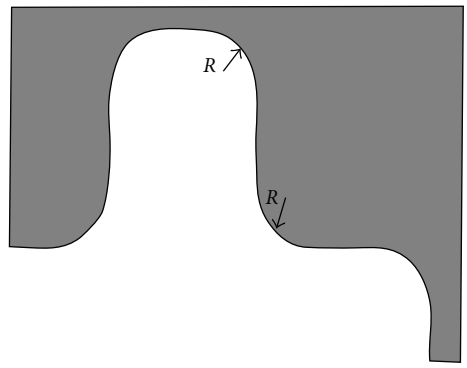

Figure 15: Partial view of a filter showing the rounded defect defined by a radius R.

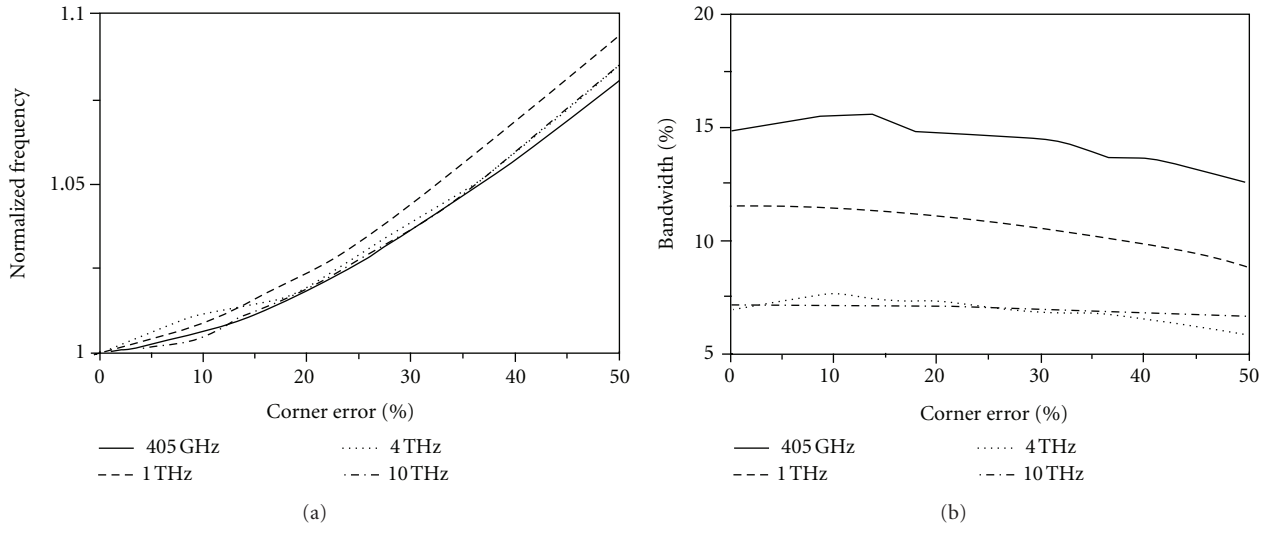

Figure 16: Effect of corner radius variation on (a) resonant frequency, (b) bandwidth.

terahertz filters, their design and fabrication process, besides of experimental results. A simple but powerful mathematical technique for designing cross filters is presented. Some useful insights can be taken from the presented parameter variation study in order to understand the mesh parameters and possible process errors influence on the filters frequency response. We conclude featuring some new companies which could provide standard and custom made filters.

Conflict of Interests

All trademarks mentioned in the paper were only cited for technical purposes and do not imply recommendation of the authors. We also indicated no potential conflict of interests.

References

[1] A. Lisauskas, T. Löffer, and G. Hartmut, "Photonics terahertz technology," *Semiconductor Science and Technology*, vol. 20, no. 7, 2005.

[2] G. P. Williams, "Filling the THz gap—high power sources and applications," *Reports on Progress in Physics*, vol. 69, no. 2, pp. 301–326, 2006.

[3] R. Appleby and H. B. Wallace, "Standoff detection of weapons and contraband in the 100 GHz to 1 THz region," *IEEE Transactions on Antennas and Propagation*, vol. 55, no. 11 I, pp. 2944–2956, 2007.

[4] H. B. Liu, H. Zhong, N. Karpowicz, Y. Chen, and X. C. Zhang, "Terahertz spectroscopy and imaging for defense and security applications," *Proceedings of the IEEE*, vol. 95, no. 8, pp. 1514–1527, 2007.

[5] H. Zhong, A. Redo, Y. Chen, and X. C. Zhang, "THz wave standoff detection of explosive materials," in *Terahertz for Military and Security Applications IV*, vol. 6212 of *Proceedings of SPIE*, Orlando, Fla, USA, April 2006.

[6] M. S. Sherwin, C. A. Schmuttenmaer, and P. H. Bucksbaum, *DOE-NSF-NIH Workshop on Opportunities in THz Science*, Arlington, Va, USA, 2004.

[7] D. W. Porterfield, J. L. Hesler, R. Densing, E. R. Mueller, T. W. Crowe, and R. M. Weikle II, "Resonant metal-mesh bandpass filters for the far infrared," *Applied Optics*, vol. 33, no. 25, pp. 6046–6052, 1994.

[8] B. Voisiat, A. Biciunas, I. Kasalynas, and G. Raciukaitis, "Bandpass filters for THz spectral range fabricated by laser ablation," *Applied Physics A*, vol. 104, no. 3, pp. 953–958, 2011.

[9] I. Puscasu, G. Boreman, R. C. Tiberio, D. Spencer, and R. R. Krchnavek, "Comparison of infrared frequency selective surfaces fabricated by direct-write electron-beam and bilayer nanoimprint lithographies," *Journal of Vacuum Science and Technology B*, vol. 18, no. 6, pp. 3578–3581, 2000.

[10] V. Nazmov, E. Reznikova, Y. L. Mathis et al., "Bandpass filters made by LIGA for the THZ region: manufacturing and testing," *Nuclear Instruments and Methods in Physics Research A*, vol. 603, no. 1-2, pp. 150–152, 2009.

[11] S. Sako, T. Miyata, T. Nakamura, T. Onaka, Y. Ikeda, and H. Kataza, "Developing metal mesh filters for mid-infrared astronomy of 25 to 40 micron," in *Advanced Optical and Mechanical Technologies in Telescopes and Instrumentation*, vol. 7018 of *Proceedings of SPIE*, Marseille, France, June 2008.

[12] S. A. Kuznetsov, V. V. Kubarev, P. V. Kalinin et al., "Development of metal mesh based quasi-optical selective components and their application in high-power experiments at Novosibirsk terahertz FEL," in *Proceedings of the FEL*, 2007.

[13] Y. Ma, A. Khalid, T. D. Drysdale, and D. R. S. Cumming, "Direct fabrication of terahertz optical devices on low-absorption polymer substrates," *Optics Letters*, vol. 34, no. 10, pp. 1555–1557, 2009.

[14] G. I. Kiani, K. P. Esselle, L. G. Olsson, A. Karlsson, and M. Nilsson, "Cross-dipole bandpass frequency selective surface for energy-saving glass used in buildings," *IEEE Transactions on Antennas and Propagation*, vol. 59, no. 2, pp. 520–525, 2011.

[15] D. W. Logan, "A frequency selective bolometer camera for measuring millimeter spectral energy distributions," Access Open Dissertations, paper 70., 2009.

[16] R. Ulrich, "Far-infrared properties of metallic mesh and its complementary structure," *Infrared Physics*, vol. 7, no. 1, pp. 37–55, 1967.

[17] P. Kaufmann, R. Marcon, A. Marun et al., "Selective spectral detection of continuum terahertz radiation," in *Millimeter, Submillimeter, and Far-Infrared Detectors and Instrumentation for Astronomy V*, vol. 7741 of *Proceedings of SPIE*, San Diego, Calif, USA, July 2010.

[18] A. M. Melo, M. A. Kornberg, P. Kaufmann et al., "Metal mesh resonant filters for terahertz frequencies," *Applied Optics*, vol. 47, no. 32, pp. 6064–6069, 2008.

[19] P. Kaufmann, "Emissões da atividade solar do submilimétrico ao infravermelho (SIRA)," FAPESP Project, 2009–2013.

[20] J. A. Bossard, L. Li, J. A. Smith et al., "Terahertz applications of frequency selective surfaces: analysis, design, fabrication and testing," in *Proceedings of the IEEE Antennas and Propagation Society International Symposium with USNC/URSI National Radio Science and AMEREM Meetings*, 2006.

[21] C. Winnewiser, F. Lewer, J. Weinzier, and H. Helm, "Transmission features of frequency selective surface compoments in the far infrared determined by terahertz time domain spectroscopy," *Applied Optics*, vol. 38, no. 18, 1999.

[22] D. H. Kim and J. I. Choi, "Design of a multiband frequency selective surface," *ETRI Journal*, vol. 28, no. 4, pp. 506–508, 2006.

[23] K. E. Paul, C. Zhu, J. C. Love, and G. M. Whitesides, "Fabrication of mid-infrared frequency-selective surfaces by soft lithography," *Applied Optics*, vol. 40, no. 25, pp. 4557–4561, 2001.

[24] G. D. Boreman, *Infrared Antennas & Frequency Selective Surfaces*, CREOL, The College of Optics & Photonics, 2011.

[25] L. A. Page, E. S. Cheng, B. Golubovic, J. Gundersen, and S. S. Meyer, "Millimeter-submillimeter wavelength filter system," *Applied Optics*, vol. 33, no. 1, pp. 11–23, 1994.

[26] H. A. Smith, M. Rebbert, and O. Sternberg, "Designer infrared filters using stacked metal lattices," *Applied Physics Letters*, vol. 82, no. 21, pp. 3605–3607, 2003.

[27] K. D. Möller, J. B. Warren, J. B. Heaney, and C. Kotecki, "Cross-shaped bandpass filters for the near- and mid-infrared wavelength regions," *Applied Optics*, vol. 35, no. 31, pp. 6210–6215, 1996.

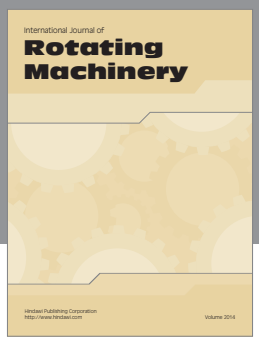

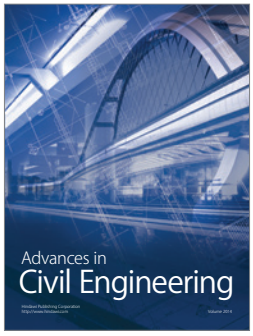

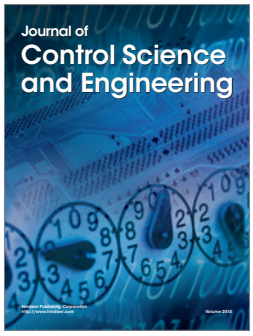

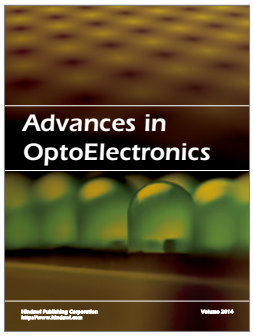

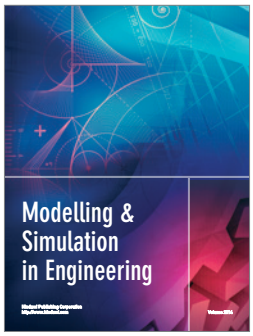

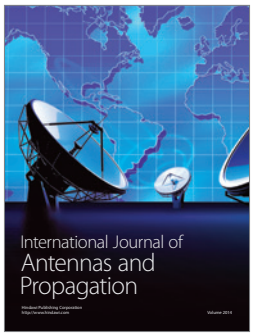

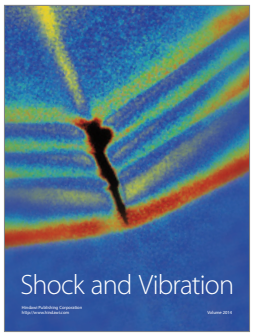

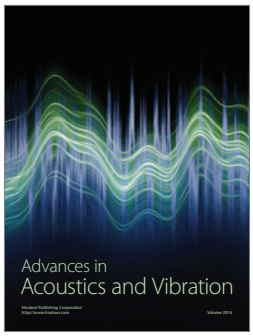

Hindawi

Submit your manuscripts at
http://www.hindawi.com